Vol 17 No 1, January 2008
1674-1056/2008/17(01)/0259-05

Chinese Physics B

Study of mechanical properties of amorphous copper with molecular dynamics simulation*

Wang Guang-Hai(王广海)[a], Pan Hui(潘 晖)[a],
Ke Fu-Jiu(柯孚久)[a)b)†], Xia Meng-Fen(夏蒙棼)[b)c)], and Bai Yi-Long(白以龙)[b)]

[a)] *Department of Physics, Beihang University, Beijing* 100083, *China*
[b)] *State Key Laboratory of Non-linear Mechanics (LNM), Institute of Mechanics, Chinese Academy of Sciences, Beijing* 100080, *China*
[c)] *Department of Physics, Peking University, Beijing* 100871, *China*

(Received 5 February 2007; revised manuscript received 28 April 2007)

The formation and mechanical properties of amorphous copper are studied using molecular dynamics simulation. The simulations of tension and shearing show that more pronounced plasticity is found under shearing, compared to tension. Apparent strain hardening and strain rate effect are observed. Interestingly, the variations of number density of atoms during deformation indicate free volume creation, especially under higher strain rate. In particular, it is found that shear induced dilatation does appear in the amorphous metal.

Keywords: molecular dynamics, amorphous, tension, shear, strain rate effect
PACC: 6220F, 6185

1. Introduction

Amorphous metals have attracted much attention since its discovery by Klement *et al*[1] due to its excellent mechanical, physical and chemical properties.[2,3] Although the macroscopic mechanical behaviour of metallic glasses has been extensively studied, the nature of the deformation mechanisms of amorphous metals remains unclear. For example, the mechanism of shear band formation is still unclear.[4−9] It is important that loading-induced change of microscopic structure of amorphous materials may affect the formation of shear band significantly. So, to reveal the structure evolution is badly needed.

One of the most useful techniques to study the mechanism is molecular dynamics simulation (MD). MD has been used to study the microscopic behaviour of materials during the transition from liquid to amorphous state.[10−13] Also, it is possible to investigate the effects of tension and shear on the microscopic mechanical behaviour of amorphous materials by using MD.[8,14]

In this paper, the transition of Cu from liquid to amorphous phase and the accompanying changes in the microscopic structure are studied by using MD. Tension and shear tests under different strain rates are simulated. Changes in the local density of atoms are studied to detect the localized structure during loading.

The paper is organized as follows. In Section 2, we discuss the model and methods. The details of our simulations and results are presented in Section 3. Section 4 gives the conclusions.

2. Model and methods

Ackland's embedded atom method (EAM) is adopted to compute potentials[15] in our simulations. Initially, 10976 Cu atoms are confined to a cube with dimensions $14\times14\times14a^3$ ($a = 0.3615\,\mathrm{nm}$, which is the lattice constant of crystalline copper). The initial velocities of atoms are assigned to follow Maxwell distribution with a specified temperature. Newton's equations of motion for the atoms in the system are numerically integrated using the Leap–Frog algorithm.[16] All simulations are performed under NPT ensemble during melting and cooling processes. Periodic boundary conditions in three dimensions are adopted in the simulations. Amorphous state is achieved by quenching the liquid Cu to 110 K at a cooling rate of $1.1\times10^{14}\,\mathrm{K/s}$.

*Project supported by the National Natural Science Foundation of China (Grant Nos 10528205, 10772012 and 10432050) and Chinese Academy of Sciences Innovation Program and KJCX2-YW-M04.
†E-mail: kefj@lnm.imech.ac.cn

We use radial distribution function[17] (RDF) $g(r)$ to analyse the structure of the metal. The meaning of RDF is that $g(r)$ represents the ratio of the number density of atoms within a spherical shell $4\pi r^2\delta r$ centred at a reference atom to the average number density of atoms. Thus, RDF can be calculated as

$$g(r) = \frac{1}{\rho_0}\frac{n(r)}{V} \approx \frac{1}{\rho_0}\frac{n(r)}{4\pi r^2\delta r}, \tag{1}$$

where ρ_0 denotes the average number density of atoms of the system, $n(r)$ is the number of atoms located in the shell from r to $r+\delta r$, and V is the volume of the shell.

In our simulations we are concerned with the mechanisms governing the tension and shear of amorphous Cu. At the top and bottom of the sample, two layers of atoms with thickness $2a$ are assumed to be 'fixed' and controlled by external loading. Free boundary conditions are enforced on the x- and y-directions. Figure 1(a) and 1(b) are the sketches for tension and shear simulations, respectively.

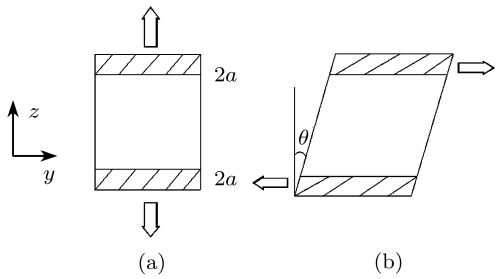

Fig.1. Tension (a) and shear (b) models with shaded regions fixed and arrowheads denoting loading direction.

3. Results and discussion

The radial distribution function exhibits a split at the second peak in the case of 110 K as shown in Fig.2. It is well known that the amorphous state is characterized by the splitting of the second peak, because it indicates the appearance of amorphous microscopic structure.[18]

The loading processes of the amorphous metal are simulated by using MD. The tensile stress–strain curves under different strain rates are plotted in Fig.3. As seen from the figure, it is clear that as strain increases, the material appears to be nonlinear and plastic with strain hardening and has a maximum stress. In addition, strain rate effects are also observed. The maximum stress increases with increasing strain rate. It can also be observed from the results that at lower strain rates, the maximum stress appears earlier. The maximum stresses and corresponding strains obtained from simulations are listed in Table 1.

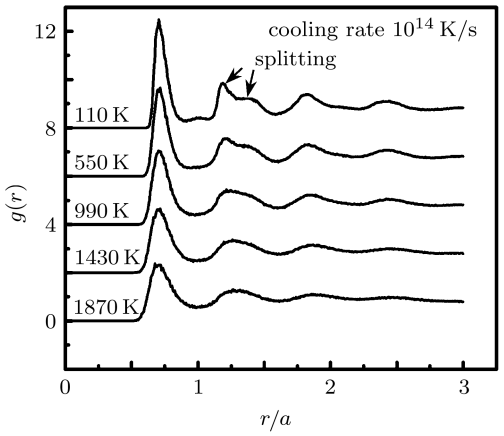

Fig.2. RDF at different temperatures.

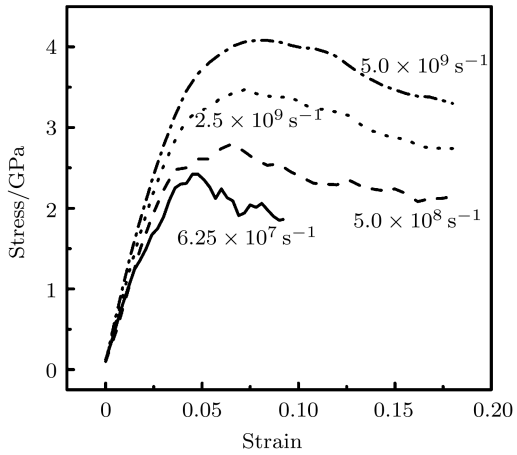

Fig.3. Tensile stress–strain curves under different strain rates.

Table 1. The maximum stresses and corresponding strains under different strain rates of tension loading.

$\dot{\varepsilon}/10^8\mathrm{s}^{-1}$	0.625	5	25	50
σ/GPa	2.40	3.00	3.47	4.08
ε	0.046	0.064	0.074	0.082

The stress–strain curves under different shear strain rates are plotted in Fig.4. In appearance, they are similar to those under tensile loading. However, the strains at which maximum shear stress appears are much greater, namely about one order greater than those under tensile loading, implying pronounced plasticity under shearing. The maximum stresses and corresponding shear strains are listed in Table 2.

Table 2. The maximum stresses and corresponding strains under different strain rates of shear loading.

$\dot{\gamma}/10^9\mathrm{s}^{-1}$	2.18	8.4	42	168
τ/GPa	4.20	4.57	5.69	6.80
γ	0.67	0.69	1.07	1.01

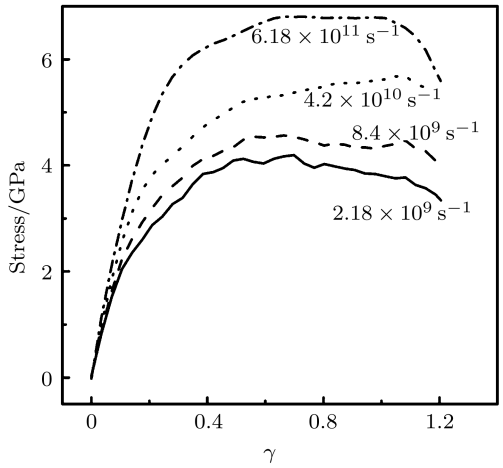

Fig.4. Stress–strain curves under different shear strain rates.

Now, we turn to the changes of microstructures of amorphous Cu during tensile and shearing loading to reveal its underlying mechanism of deformation. Spapen[19] described the deformation process in metallic glasses as a competition between stress-driven creation and diffusion annihilation of free volume. On the other hand, the free volume should be defined as the excess volume surrounding an atom relative to the volume surrounding an atom in a perfect crystal. So, the free volume can be calculated as the change of number density of atoms.

In our simulations, there are some microstructural differences observed at different strains under different strain rates. We calculated the local number density of atoms by counting the atoms in the neighbourhood of any specified atom. To define neighbourhood, we defined a cutting radius of $1.9\,a$, namely the cutting radius in potential function.

The distributions of number density at strain rate $\dot{\varepsilon} = 5 \times 10^9\mathrm{s}^{-1}$ under tension are plotted in Fig.5(a) for $\varepsilon = 0$ and $\varepsilon = 0.0408$, respectively. The strain $\varepsilon = 0.0408$ corresponds to the strain at maximum stress. Two peaks of number density can be seen in Fig.5(a). As the stress increases to the maximum, both peaks shift to the left, indicating lower number density, i.e. free volume creation, owing to tensile deformation. On the other hand, it is known that shear deformation usually keeps the volume unchanged. However, in our simulations we found that the phenomenon of leftward peak shift in tension also appears under shear loading as shown in Fig.5(b).

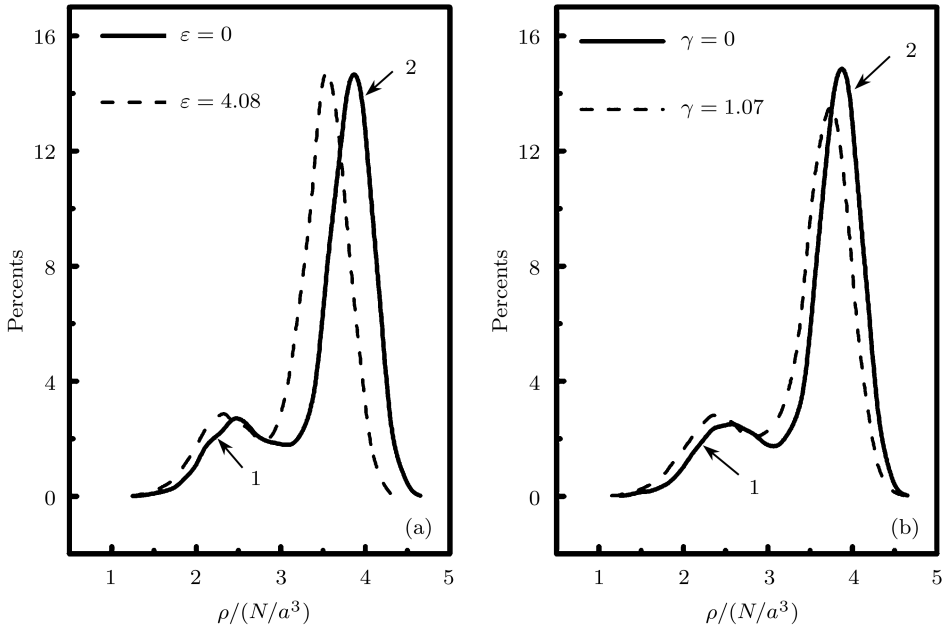

Fig.5. (a) Distributions of number density at strain rate $\dot{\varepsilon} = 5\times10^9\mathrm{s}^{-1}$ and strains $\varepsilon = 0$ (solid line), and $\varepsilon = 0.0408$ (dashed line), respectively, in tension. (b) Distributions of number density at shear strain rate $\dot{\gamma} = 4.2 \times 10^{10}\mathrm{s}^{-1}$, and shear strains $\gamma = 0$ (solid line), and $\gamma = 1.07$ (dash line), respectively.

This demonstrates that shear induced dilatation does appear in the amorphous metal. The distributions of number density under different strain rates but at the same strain are plotted in Figs.6(a) and 6(b) for tension and shear, respectively. Compared with the case of lower strain rate, the peak of number density under higher strain rate are located more to the left. This may indicate more free volume being created under higher strain rate.

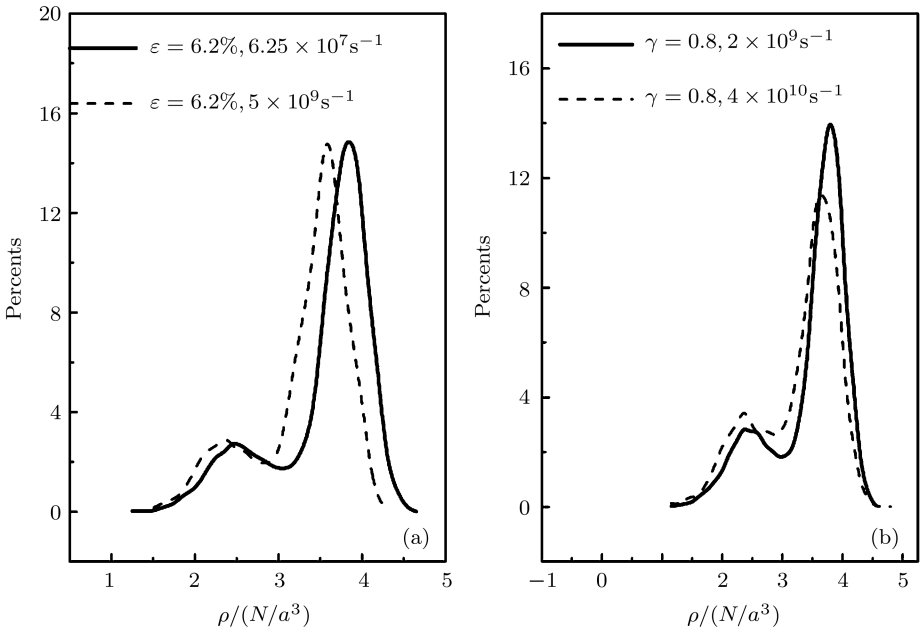

Fig.6. Distribution of number density under different strain rates for (a) tension at strain rates $\dot{\varepsilon} = 6.25 \times 10^7 \mathrm{s}^{-1}$ (solid line) and $\dot{\varepsilon} = 5 \times 10^9 \mathrm{s}^{-1}$ (dashed line) at the same strain $\varepsilon = 0.062$, and (b) at shear strain rates $\dot{\gamma} = 2 \times 10^9 \mathrm{s}^{-1}$ (solid line) and $\dot{\gamma} = 4 \times 10^{10} \mathrm{s}^{-1}$ (dashed line) at the same shear strain $\gamma = 0.8$.

So, as shown in Figs.5 and 6, corresponding to the decrease of density,[20] additional free volume is generated during deformation. Also, since atoms can not relax fully under higher strain rate, the stress becomes higher. Hence strain rate effect could be originating from the competition between relaxation and work hardening.

4. Conclusions

In summary, the formation of amorphous copper and its mechanical properties under different strain rates are studied by using molecular dynamics simulation. The results of tension and shear show that plastic deformation with strain hardening and strain rate effect are produced. However, compared with tensile deformation, pronounced plasticity is found under shearing. Interestingly, the distribution of number density of atoms shifts to the lower side during deformation, indicating free volume creation. Additionally, under higher strain rate, the peak of number density distribution shifts to the left of that at lower strain rate, indicating more free volume being generated at higher strain rate. In particular, it is found that the phenomenon of leftward peak shift also appears under shear loading. This demonstrates that shear induced dilatation does appear in the amorphous metal.

References

[1] Klement W, Willens R and Duwez P 1960 *Nature* **187** 869
[2] Wang W H 2004 *Mater. Sci. Eng.* R **44** 45
[3] Meng Q G, Li J G and Zhou J K 2006 *Chin. Phys.* **15** 1549
[4] Dai L H, Yan L M, Liu F and Bai Y L 2005 *Appl. Phys. Lett.* **87** 141916
[5] Liu L F, Dai L H, Bai Y L, Wei B C and Eckert J 2005 *Mater. Chem. Phys.* **93** 174
[6] Masato Shimono and Hidehiro Onodera 2001 *Mater. Sci. Eng.* A **304** 515
[7] Falk M L and Langer J S 1998 *Phys. Rev.* E **57** 7192

[8] Nicholas P B, Jakob SchiØtz and Jacobsen W 2006 *Phys. Rev.* B **73** 064108
[9] Wang J F, Liu L, Pu J and Xiao J Z 2004 *Acta Phys. Sin.* **53** 1916 (in Chinese)
[10] Nicholas P B 2004 *Phys. Rev.* B **69** 144205
[11] Li H and Wang G H 2002 *J. Chem. Phys.* **116** 10809
[12] Zhang L, Wang S Q and Ye H Q 2006 *Chin. Phys.* **15** 0610
[13] Zhu C Z, Zhang P X, Xu Q M, Liu J H, Ren X Z, Hong W L and Li L L 2006 *Acta Phys. Sin.* **55** 4795 (in Chinese)
[14] Li Q K and Li M 2006 *Intermetallics* **14** 1005
[15] Ackland G J and Vitek V 1990 *Phys. Rev.* B **41** 10324
[16] Zhou X W, Wadlcy H N G and Johnson R A 2001 *Acta Mater.* **49** 4005
[17] Ciccotti G, Guillope M and Pontikis V 1983 *Phys. Rev.* B **27** 5576
[18] Li G X and Liang Y F 2003 *J. Phys.*: *Condens. Matter* **15** 2259
[19] Spapen F 1977 *Acta Metall.* **25** 40
[20] Wang G H, Pan H, Ke F J, Xia M F and Bai Y L 2007 *J. Beijing University of Aeronautics and Astronautics* **33** 752